

Numerical simulation of sheet metal forming processes using a new yield criterion

Dan-Sorin COMSA^{1, a}, Dorel BANABIC^{1, b}

¹Technical University of Cluj-Napoca, Department of Manufacturing Engineering,

Bd. Muncii nr. 103-105, 400641 Cluj-Napoca, Romania

^adscomsa@tcm.utcluj.ro, ^bbanabic@tcm.utcluj.ro

Keywords: Sheet metal forming, finite element simulation, yield criterion

Abstract. The paper is focused on the development of a new phenomenological yield criterion able to describe the inelastic response of sheet metals subjected to cold forming. The model consists in two components: the equivalent stress and the hardening law. The equivalent stress is a function incorporating 8 material parameters. Due to these parameters, the new formulation is able to describe four normalized yield stresses (y_0, y_{45}, y_{90}, y_b) and four coefficients of plastic anisotropy (r_0, r_{45}, r_{90}, r_b). The hardening law is defined as a linearly asymptotic function containing 4 material parameters. The numerical tests presented in the last section of the paper prove the capability of the elastoplastic constitutive models based on the new yield criterion to model the earing as well as the wrinkling phenomena accompanying the deep-drawing process.

Introduction

The yield criterion is an essential component of the mechanical models used for simulating sheet metal forming processes. Its capability to describe the plastic anisotropy has a major influence on the quality of the numerical results. The authors have developed a yield criterion for orthotropic sheet metals subjected to cold forming. The new formulation has been included in an elastoplastic constitutive model and implemented as a UMAT routine in the commercial finite element code LS-DYNA [1]. A set of NUMISHEET 2002 [2] benchmark tests (deep-drawing of a cylindrical cup with high and low blank holding force, respectively) will be used to prove the performances of the yield criterion.

Formulation of the New Yield Criterion

The basic component of the plasticity model used in our approach is the yield surface [3]:

$$\Phi(\bar{\sigma}, Y) := \bar{\sigma} - Y = 0, \quad (1)$$

where $\bar{\sigma}$ is the equivalent stress and Y is a yield parameter. $\bar{\sigma}$ is a scalar quantity defined as a dependency of the non-zero stress components $\hat{\sigma}_{11}, \hat{\sigma}_{22}$, and $\hat{\sigma}_{12} = \hat{\sigma}_{21}$ (expressed in an orthonormal basis having the same orientation as the local orthotropy axes):

$$\bar{\sigma} = \bar{\sigma}(\hat{\sigma}_{11}, \hat{\sigma}_{22}, \hat{\sigma}_{12} = \hat{\sigma}_{21}). \quad (2)$$

Another element of the plasticity model is the flow rule associated to the yield surface [3]. Assuming a purely isotropic hardening of the material, only one scalar state parameter is needed to describe the evolution of the yield surface. This parameter is the equivalent plastic strain $\bar{\epsilon}^p$ [3]. The change of the yield surface is included in equation (1) by means of the hardening law [3]:

$$Y = Y(\bar{\epsilon}^p). \quad (3)$$

We propose the following formulations for the terms included in Eq. 1:

- Equivalent stress

$$\bar{\sigma} = \left[p_1 (L+M)(cL+M)(L+cM) + p_2 (L+N)(cL+N)(L+cN) \right]^{1/6},$$

$$L(\hat{\sigma}_{11}, \hat{\sigma}_{22}, \hat{\sigma}_{12} = \hat{\sigma}_{21}) = (p_3 \hat{\sigma}_{11} - p_4 \hat{\sigma}_{22})^2 + \hat{\sigma}_{12} \hat{\sigma}_{21},$$

$$M(\hat{\sigma}_{11}, \hat{\sigma}_{22}, \hat{\sigma}_{12} = \hat{\sigma}_{21}) = (p_5 \hat{\sigma}_{11} - p_6 \hat{\sigma}_{22})^2 + \hat{\sigma}_{12} \hat{\sigma}_{21}, \quad (4)$$

$$N(\hat{\sigma}_{11}, \hat{\sigma}_{22}) = (p_7 \hat{\sigma}_{11} + p_8 \hat{\sigma}_{22})^2,$$

$$c = (2 + \sqrt{3})^2, \quad p_1, \dots, p_8 > 0.$$

- Hardening law

$$Y = q_1 + (q_2 + q_3 \bar{\epsilon}^p) \arctan(q_4 \bar{\epsilon}^p), \quad q_1 > 0, q_2 > 0, q_3 \geq 0, q_4 > 0. \quad (5)$$

The quantities p_1, \dots, p_8 (see Eq. 4) and q_1, \dots, q_4 (see Eq. 5) are material parameters¹. The identification procedure of the equivalent stress involves the numerical solution of a non-linear set of equations enforcing 8 constraints on the shape of the yield surface [4]:

$$\begin{aligned} \tilde{Y}_\theta(p_1, \dots, p_8) &= y_\theta, & \tilde{r}_\theta(p_1, \dots, p_8) &= r_\theta, & \theta &= 0^\circ, 45^\circ, 90^\circ, \\ \tilde{Y}_b(p_1, \dots, p_8) &= y_b, & \tilde{r}_b(p_1, \dots, p_8) &= r_b \end{aligned} \quad (6)$$

($\tilde{Y}_\theta, \tilde{Y}_{45}, \tilde{Y}_{90}, \tilde{Y}_b, \tilde{r}_\theta, \tilde{r}_{45}, \tilde{r}_{90}, \tilde{r}_b$ - predicted values; $y_\theta, y_{45}, y_{90}, y_b, r_\theta, r_{45}, r_{90}, r_b$ - experimental values of the uniaxial/equibiaxial normalised yield stresses and coefficients of plastic anisotropy, respectively). By using both uniaxial and equibiaxial material data, the equivalent stress is able to provide an accurate description of the plastic anisotropy of sheet metals.

The identification procedure of the hardening law is based on the least-square minimisation of the error-function [4]

$$f(q_1, \dots, q_8) = \sum_{i=1}^n \left\{ q_1 + (q_2 + q_3 {}^{(i)}\bar{\epsilon}^p) \arctan(q_4 {}^{(i)}\bar{\epsilon}^p) - {}^{(i)}Y \right\}^2, \quad (7)$$

where $\{ {}^{(i)}\bar{\epsilon}^p, {}^{(i)}Y \mid i = 1, \dots, n \}$ is a set of points selected from an experimental hardening diagram.

Implementation of the New Yield Criterion in an LS-DYNA Elastoplastic Constitutive Model

In the LS-DYNA [1] implementation of the constitutive model, the sheet metal has been treated as a thin elastoplastic shell with purely elastic bending response. Due to the small amount of recoverable strains [3], the deformation can be considered as being isochoric. A linearly isotropic constitutive model has been associated to the elastic component of the strain tensor. The new yield criterion and its associated flow rule presented in the previous section of the paper have been used to describe the plastic behaviour of the sheet metal. We have assumed that the local axes of plastic orthotropy change continuously during the forming process (the rotational component of the deformation gradient tensor defining their current orientation).

¹ The yield surface defined by Eqs. 1 and 4 is always convex in the stress space if $p_1, \dots, p_8 > 0$ [4].

Performances of the New Yield Criterion. Comparison with the NUMISHEET 2002 Deep-Drawing Benchmark Data

A couple of benchmark tests proposed by the organisers of the NUMISHEET 2002 conference will be used to evaluate the performances of the new yield criterion (see Table 1).

Table 1. NUMISHEET 2002 benchmark tests (<http://www.numisheet2002.org/benchmarks.html>)

Description of the benchmark test	Source of the experimental data used for comparison
Deep-drawing of a cylindrical cup – high blank holding force of 50 kN (AA6111-T4 sheet metal; 1 mm thickness)	File Report_A_AE01.xls in the NUMISHEET 2002 database
Deep-drawing of a cylindrical cup – high blank holding force of 10 kN (AA6111-T4 sheet metal; 1 mm thickness)	

As we can see in Table 1, both tests make reference to the same sort of sheet metal. The constitutive model implemented in LS-DYNA describes the elastoplastic behaviour of the material using the parameters listed in Table 2.

Table 2. Parameters of the constitutive model² (AA6111-T4 sheet metal; 1 mm thickness)

Elasticity parameters	Young's modulus E [MPa]	70500
	Poisson's ratio ν	0.342
Parameters of the equivalent stress (see Eq. 4)	p_1	0.053909
	p_2	0.183283
	p_3	0.472031
	p_4	0.476445
	p_5	0.565157
	p_6	0.539226
	p_7	0.392415
	p_8	0.453192
Parameters of the hardening law (see Eq. 5)	q_1 [MPa]	186.595155
	q_2 [MPa]	162.649605
	q_3 [MPa]	54.195452
	q_4	11.022298

The frictional parameters used in the numerical tests (defined in the NUMISHEET 2002 database) are listed in Table 3.

Table 3. Parameters of the frictional contact (AA6111-T4 sheet metal; 1 mm thickness)

Characteristics of the frictional contact	Coulomb frictional coefficient μ
Dry friction	0.1348
Friction in the presence of an FD-1500 lubricant	0.0096

²The parameters defining the plastic behaviour of the sheet metal have been computed using raw material data provided by ALCOA (http://www.numisheet2002.org/M1_Raw.zip).

The set-up of the NUMISHEET 2002 deep-drawing benchmarks is shown in Fig. 1. In both cases, the punch stroke is 40 mm. The numerical data used for comparison with the experimental results are listed below:

- Punch force vs. punch displacement diagram
- Earing profile in the case of the high blank-holding force (Fig. 2.a) and wrinkle amplitude in the case of the low blank-holding force (Fig. 2.b)
- Thickness distribution in three axial planes defined by 0° , 45° and 90° angles measured with respect to the rolling direction (RD).

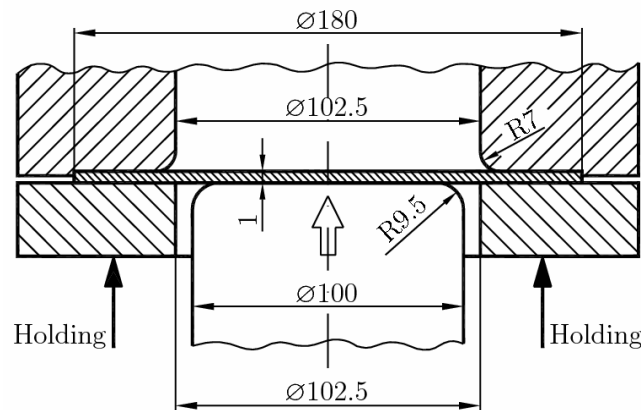


Figure 1. Set-up of the NUMISHEET 2002 deep-drawing benchmarks (AA6111-T4 sheet metal; 1 mm thickness)

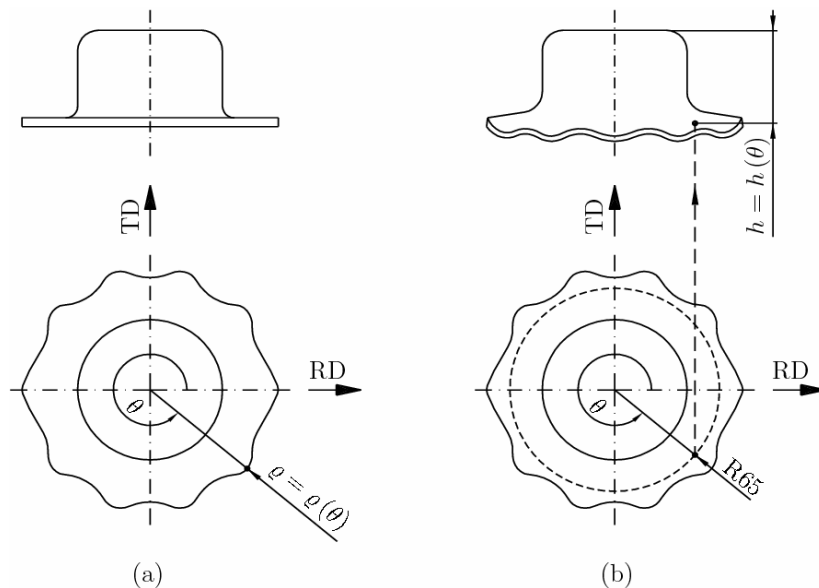


Figure 2. NUMISHEET 2002 deep-drawing benchmarks - characteristics of the flange (AA6111-T4 sheet metal; 1 mm thickness)

Due to the plastic orthotropy of the sheet metal, only one quarter of the blank has been meshed using 2876 Belytschko-Lin-Tsai shells [1] with 3 Gauss-Legendre integration points along the thickness. The active surfaces of the tools have been described as collections of VDA patches [1]. The dynamic explicit computational scheme with uniform mass scaling [1] has been adopted for simulating both deep-drawing processes.

The diagrams shown in Figs 3 – 9 provide a comparison between the numerical results and the experimental data.

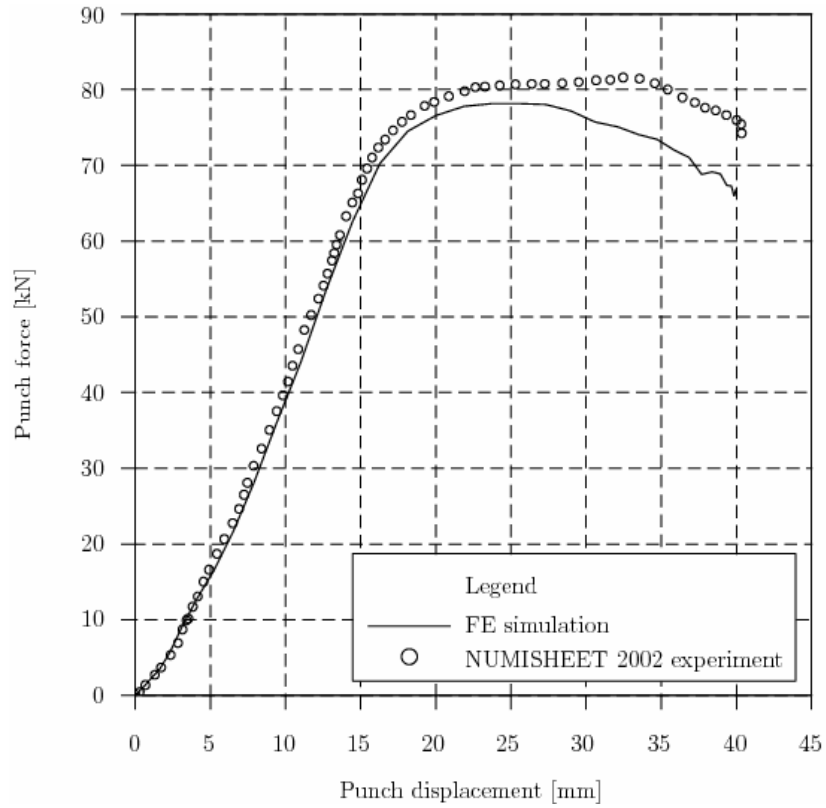


Figure 3. Evolution of the punch load: NUMISHEET 2002 deep-drawing benchmark – high blank-holding force (AA6111-T4 sheet metal; 1 mm thickness)

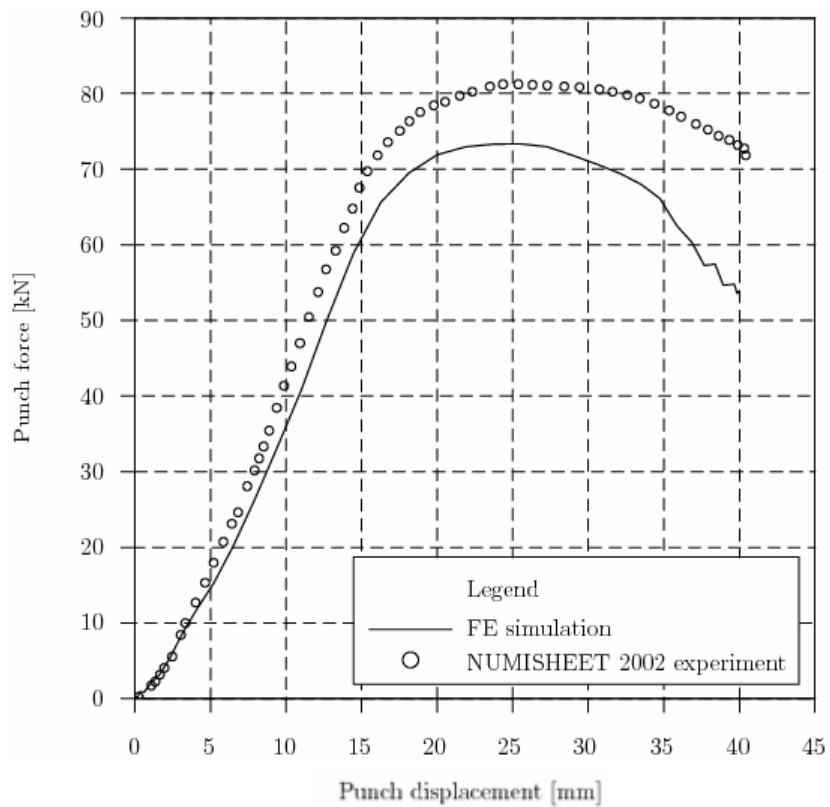


Figure 4. Evolution of the punch load: NUMISHEET 2002 deep-drawing benchmark – low blank-holding force (AA6111-T4 sheet metal; 1 mm thickness)

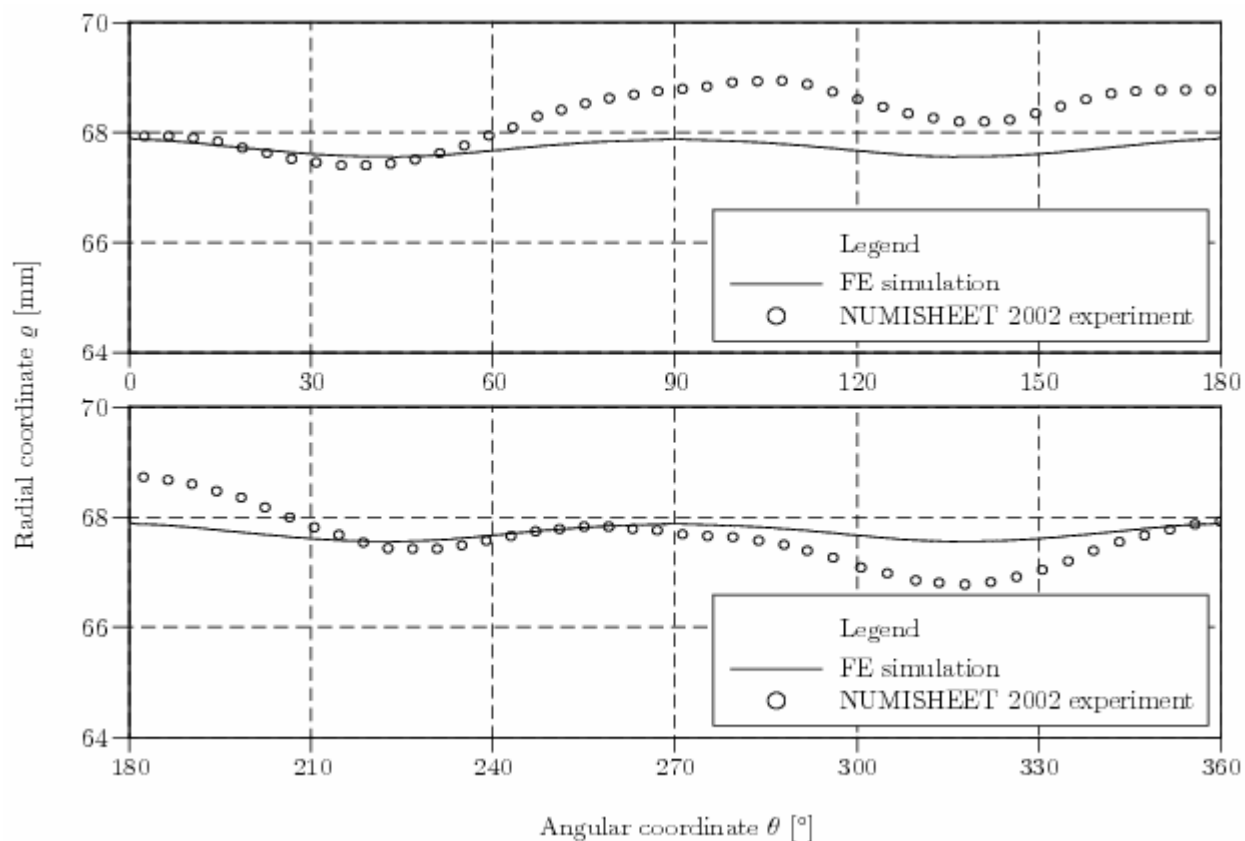


Figure 5. Earing profile: NUMISHEET 2002 deep-drawing benchmark – high blank-holding force (AA6111-T4 sheet metal; 1 mm thickness)

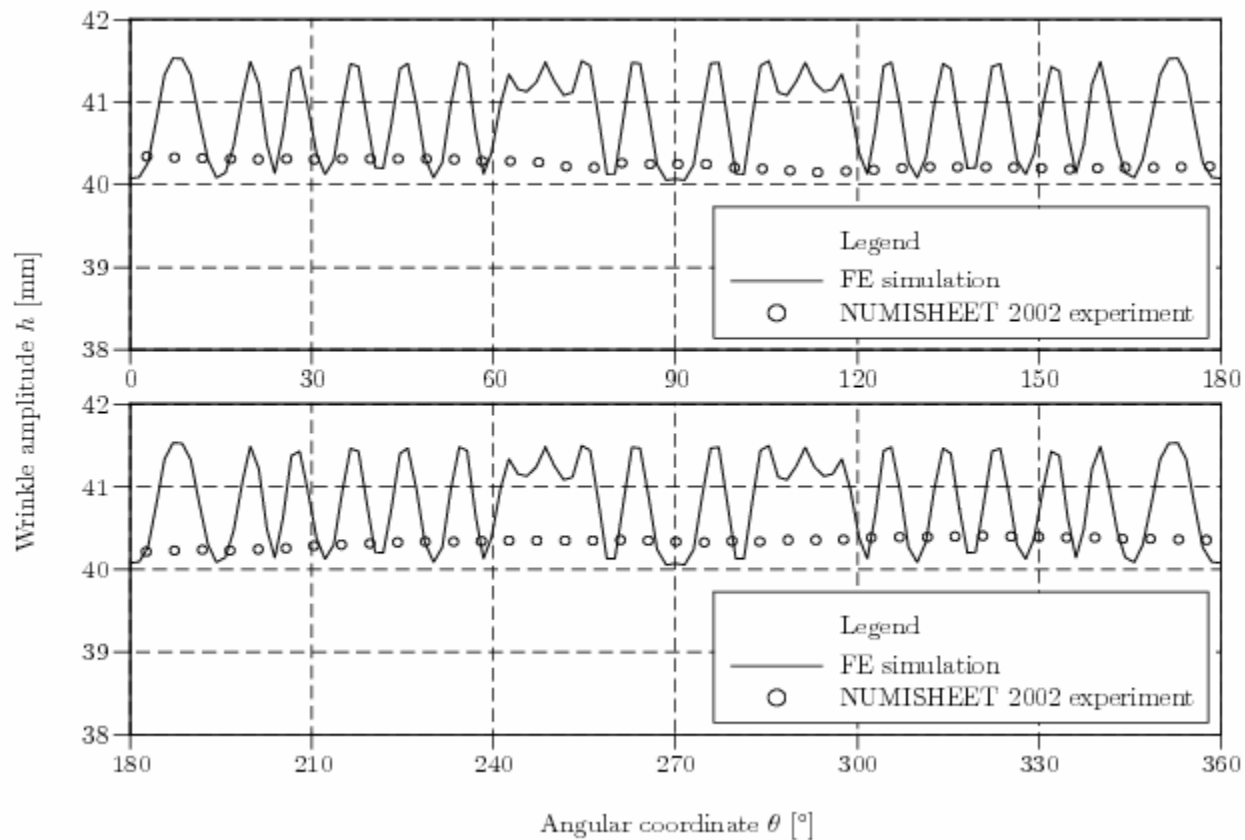


Figure 6. Wrinkle amplitude: NUMISHEET 2002 deep-drawing benchmark – low blank-holding force (AA6111-T4 sheet metal; 1 mm thickness)

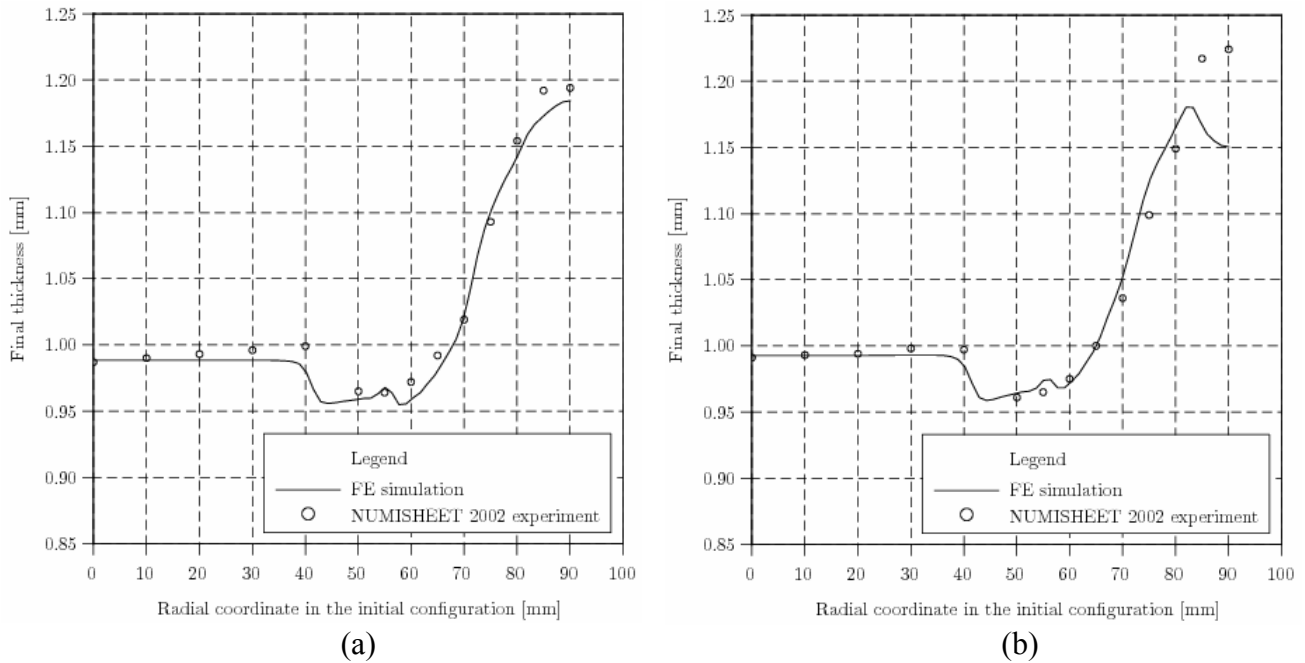


Figure 7. Final thickness of the cup wall in an axial plane defined by a 0° angle measured with respect to the rolling direction: NUMISHEET 2002 deep-drawing benchmark – (a) high blank-holding force; (b) low blank-holding force (AA6111-T4 sheet metal; 1 mm thickness)

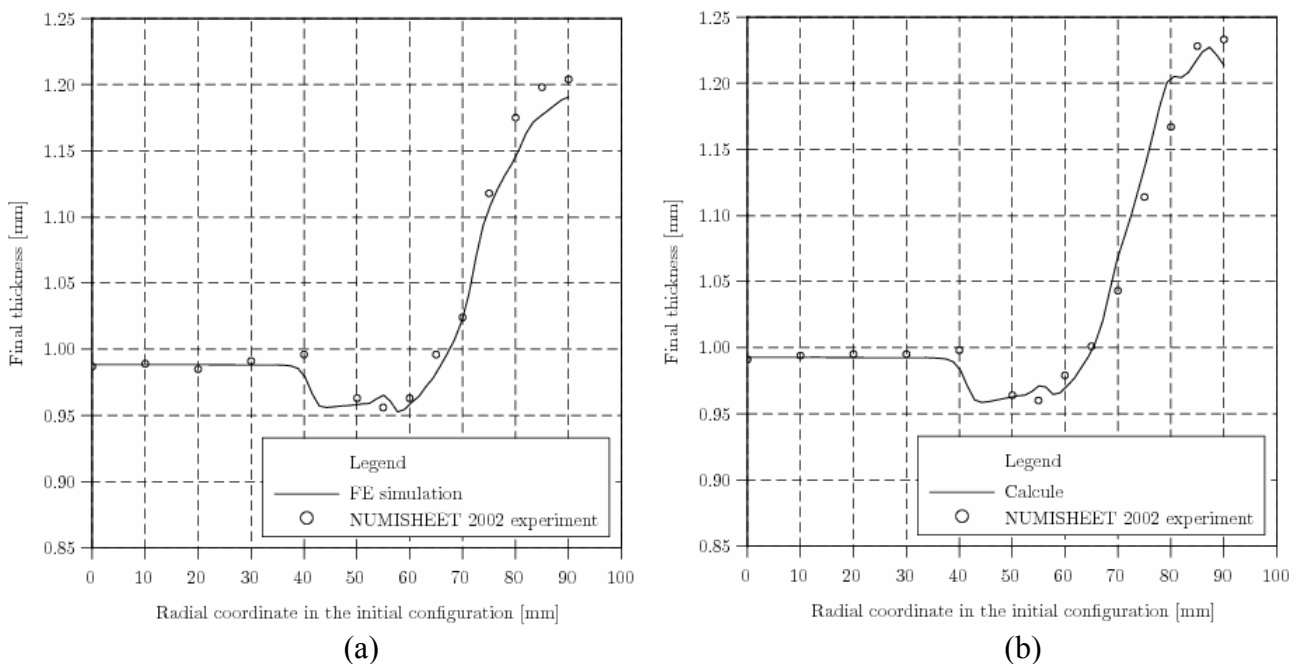


Figure 8. Final thickness of the cup wall in an axial plane defined by a 45° angle measured with respect to the rolling direction: NUMISHEET 2002 deep-drawing benchmark – (a) high blank-holding force; (b) low blank-holding force (AA6111-T4 sheet metal; 1 mm thickness)

As one may expect, the agreement between computation and experiment is better in the case of the high blank-holding force benchmark. The quality of the punch force vs. punch displacement diagram (Fig. 3) is the first aspect that should be noticed. Even if not being superimposed on the experimental points, the calculated curve gives a very good prediction of the maximum load. In our opinion, the discrepancies that can be observed along the descending region of the curve are mainly caused by the approximations included in the contact algorithm of the finite-element code [1].

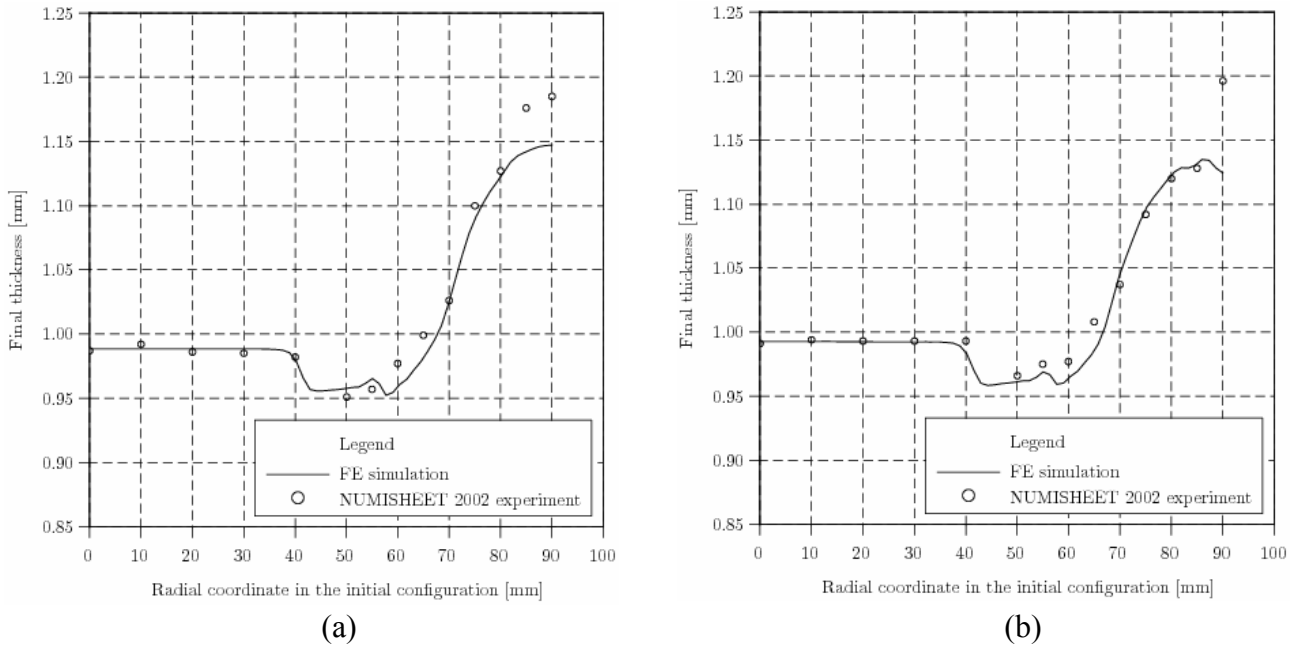


Figure 9. Final thickness of the cup wall in an axial plane defined by a 90° angle measured with respect to the rolling direction: NUMISHEET 2002 deep-drawing benchmark – (a) high blank-holding force; (b) low blank-holding force (AA6111-T4 sheet metal; 1 mm thickness)

The distribution of the experimental points defining the earing profile (Fig. 5) is not rigorously orthotropic. In this case, the computational errors are mainly due to the constitutive model. But, as we can see, the differences are not very important. In fact, the numerical result is a very good average of the measured earing. The thickness predictions are also satisfactory in the case of the high blank-holding force benchmark (see Figs. 7.a, 8.a and 9.a). The discrepancies that can be observed on the diagram corresponding to the 90° axial plane (Fig. 9.a) are surely generated by the orthotropy hypothesis included in the constitutive model. In the case of the low blank-holding force benchmark, a number of 43 wrinkles have been put into evidence by the experiment. The finite-element model predicts 42 wrinkles (Fig. 6). Due to the fact that their amplitude is not very accurately described, the quality of the other numerical results (especially the thickness distribution in the flange area – see Figs. 7.b, 8.b and 9.b) is poorer. However, for practical purposes, the capability of the model to give a good prediction of the wrinkle occurrence is the most important.

Conclusions

The yield criterion has a major influence on the quality of the numerical results obtained when simulating sheet metal forming processes. As shown by the tests presented in this paper, the predictions of the models able to give a better description of the anisotropy and strain hardening are in a very satisfactory agreement with experimental data.

References

- [1] J.O. Hallquist: *LS-DYNA Theoretical Manual* (Livermore Software Technology Corp. 1998).
- [2] D.Y. Yang, S.I. Oh, H. Huh and Y.H. Kim (eds.): *Proc. of NUMISHEET 2002 Conference* (Jeju Island, Korea 2002).
- [3] R. Hill: *The Mathematical Theory of Plasticity* (Clarendon Press, Oxford 1950).
- [4] D.S. Comsa: *Numerical Simulation of Sheet Metal Forming Processes Using a New Yield Criterion. PhD Thesis – in Romanian* (Technical University of Cluj-Napoca, Romania 2006).